Desalination and Water Treatment
www.deswater.com
doi: 10.5004/dwt.2020.25024

179 (2020) 45–53
March

Formation and properties of pure-oxygen aerobic granular sludge (POAGS) at high organic loading rates (HOLR)

Fanghui Pan[a,b], Youbao Wang[a,c,*], Yongbin Jiang[b,d], Xinxi Zhang[b,e], Kunxiao Huang[d], Tibamba Matthew[a,f]

[a]*College of Life Sciences, Anhui Normal University, Wuhu 241000, Anhui, China, Tel. +86-553-3869193; emails: wyb74@126.com (Y. Wang), pfh20072008@126.com (F.H. Pan), ntilichemi@gmail.com (T. Matthew)*
[b]*Engineering Research Center of Biomembrane Water Purification and Utilization Technology of Education, Anhui University of Technology, Ma'anshan 243032, Anhui, China, emails: yongbin_jiang@163.com (Y.B. Jiang), zhang-xinxi@163.com (X.X. Zhang)*
[c]*Anhui Provincial Key Lab. of the Conservation and Exploitation of Biological Resources, Anhui Normal University, Wuhu 241000, Anhui, China*
[d]*Department of Environmental Science and Engineering, Anhui University of Technology, Ma'anshan 243032, Anhui, China, email: huangkunxiao1988@126.com*
[e]*Department of Civil Engineering, Anhui University of Technology, Ma'anshan 243032, Anhui, China*
[f]*Department of Science, Dambai College of Education, Dambai, Ghana*

Received 25 April 2019; Accepted 13 October 2019

ABSTRACT

Although aerobic granular sludge (AGS) and pure-oxygen aeration techniques have significant merits for treating wastewater, the formation and relative properties of AGS with pure-oxygen aeration treating high organic loading rates (HOLR) wastewater are still inconclusive. Therefore, the physiochemical and biochemical properties of pure-oxygen AGS (POAGS) treating HOLR wastewater compared with air AGS (AAGS) were explored. The results indicated that the average removal rate of COD and NH_4^+–N in POAGS were 22% and 14% higher than those in AAGS, respectively, when mean influent loading of COD and NH_4^+–N were at 2.9 and 0.18 kg m^{-3} d^{-1}. The settling velocity of POAGS was three times faster than that of AAGS, implying POAGS with more excellent solid–liquid separation. X-ray fluorescence result indicated formation of POAGS demands less Ca^{2+} addition and eliminates more P in wastewater. Optical microscope and scanning electron microscope analysis showed that POAGS has a denser and more compact structure compared with AAGS, which could aggregate multi-species communities secreting abundant viscous EPS to endure HOLR and maintain high removal efficiency and good settleability. It was further speculating that the combined action of adequate dissolved oxygen and rich nutrient was a prerequisite for the formation of excellent biochemical properties in POAGS.

Keywords: Pure-oxygen aerobic granular sludge; Compact structure; Influent loading shock; Excellent solid–liquid separation; High organic loading rates

1. Introduction

High organic loading wastewater treatment is still a challenging issue for researchers, due to its characteristics of complex components, high concentration of COD, NH_4^+–N and SS, and difficult for degradation [1,2]. Although physical–chemical and biological methods are capable of disposing high organic loading wastewater [1,3], an economical and effective method with no secondary pollution for the high organic loading wastewater treatment is urgent to be explored presently.

* Corresponding author.

Aerobic granular sludge (AGS) is regarded to be promising in the field of wastewater treatment [4–6], due to its regular, dense and strong microbial structure, outstanding settling ability and stability at high organic loading rates (HOLR) [7–12]. Thanh et al. [13] have reported that AGS was capable of resisting high organic loading shock, maintaining good effluent performance and fast settling velocity. Caudan et al. [14] have demonstrated the roles of extracellular polymeric substances (EPS) for AGS formation and stability in wastewater treatment experiment.

Dissolved oxygen (DO) played a critical role in treating high organic loading wastewater [15]. Low DO concentrations resulting in excessive filamentous bacterial growth, sludge exhibited poor settling properties and poor effluents with high turbidities, as using conventional air aeration [16–19]. Pure oxygen aeration is the capacity to offer adequate DO to improve biomass activity and sludge settleability [20–23], and control volatile organic compounds and odors emission [24,25].

It is worth mentioning that pure oxygen aeration technology could save energy and cost [26–28]. The technology has become commercialized in the United Sates since 1970 [15,29]. It was nearly 30% energy to be saved, as compared with traditional air aeration technology [29,30]. Relevant statistical data indicated that electrical power consumption of high-purity-oxygen activated sludge process roughly at 0.35 kW h m^{-3}, but the energy depletion for air aeration process around at 1.70 kW h m^{-3} [31,32]. That is to say, a 1.5×10^5 t d^{-1} wastewater treatment plant could save electric energy closely to 2.8×10^6 kW h and reduce the annual operation cost about at 2.5×10^5 dollar of operating cost yearly [31,32].

To date, most research works on AGS has generally focused on treating wastewater at conventional air aeration. However, little studies have used AGS for treating HOLR wastewater at pure oxygen aeration. Therefore, the main object of this study was to cultivate POAGS at HOLR and to observe its resistance to influent shock loading and settleability through correlation analysis of influent concentration with effluent concentration and settle curves tests, as well as its biochemical properties in terms of microstructure, mineral composition, functional groups using optical microscope, energy dispersive X-ray (EDX) technique coupled with scanning electron microscope (SEM), X-ray fluorescence (XRF) and FTIR. Further, the potential causes of biochemical properties of POAGS were revealed according to DO transfer and elastic swelling and shrinkage of viscous EPS. Air aerobic granular sludge (AAGS) was cultivated and designed as control experiment.

2. Methods and materials

2.1. Experimental set-up

The experimental setup consisted of two bench-scale sequencing batch reactor systems (Fig. 1). The reactors of R1 and R2, with an inner diameter of 110 mm and the working volume of 7.6 L, were used. In this experiment, R1 was supplied with pure oxygen aeration and R2 was used with air aeration. Process batch cycles of 510 min length were established as follows: feed (10 min), aerobic reaction (480 min), settling (10 min), withdraw (10 min). Hydraulic retention time was fixed approximately at 7.9 h, with a volumetric exchange ratio of 70%. The sludge retention time was about 21 h in R1 and R2. The inlet was at the top the reactor and the outlet at one third location up to the bottom reactor. The gas flow rate into R1 and R2 was about 0.5 L min^{-1}, which allowed DO concentration to be maintained around 6.5 mg L^{-1} in R1 and around 2 mg L^{-1} in R2.

2.2. Cultivation

The seed sludge was taken from a local municipal wastewater treatment plant in Ma'an Shan city, China. The sludge was mixed with sewage in accordance with volume ratio of 1:2 into the reactors. The initial mixed liquid suspended solid (MLSS) and sludge volume index (SVI) was separately at about 3.3 g L^{-1} and 95 mL g^{-1} in R1 and R2.

A synthetic wastewater was made up of mixture of raw wastewater and extra substrates for sludge cultivation to

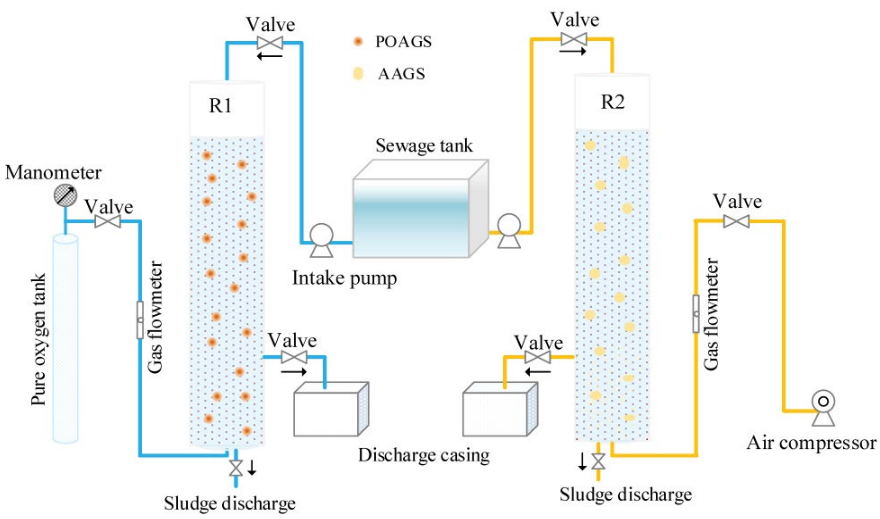

Fig. 1. Schematic diagram of lab-scale SBR systems for cultivating POAGS and AAGS.

form POAGS and AAGS. The raw wastewater was taken from a sewage tank in the campus (Anhui University of Technology). The extra substrates were added into the raw wastewater. The substrate composition and concentration are shown in Table 1. Additionally, influent concentration and influent loading in the two reactors are also exhibited in Table 1.

2.3. Conventional index analysis

The samples were collected from the two reactors at the end of each cycle. COD, NH_4^+–N, MLSS and SVI were measured in each cycle according to Standard Methods [33]. Correlation between influent concentration and effluent concentration in terms of COD and NH_4^+–N was further fitted and analyzed. The settling curves were determined using the method described by Zhang et al. [34] and Schuler and Jang [35]. The DO concentration was monitored at each reaction in the two reactors using portable DO meter (JPBJ-608). The EPS of granules were determined 10 times during mature stage, according to polysaccharide and protein content of samples from each cycle. Each sample was duplicated triplicate. The EPS was extracted with a heat extraction method [36]. The polysaccharide content in EPS was measured using the phenol-sulphuric acid method with glucose as the standard; the protein content in EPS was measured using the Lowry method with bovine serum albumin as the standard [12].

2.4. Micromorphology, functional group and elements analysis

The morphology of seed sludge flocs and granular sludge formed was observed daily in an optical microscope (Phenix ME200) equipped with an eyepiece micrometer for average floc size estimation. The images of mature granules were captured by a digital camera (SONY, DSC-W730, Japan). The microbial compositions of granules were observed qualitatively and the mineral elements from surface layer of granules were determined quantitatively using EDX technique coupled with scanning electron microscope (SEM; JSW-6490LW). The mineral elements of granules and sludge were measured qualitatively and quantitatively using (XRF (ARLAdant'X Intellipower™ 3600, Thermo Fisher, America). The functional groups of granules were measured using Fourier transform infrared spectroscopy (FTIR) (Nicolet 6700, America).

3. Results and discussion

3.1. Resistance of POAGS to influent shock loading

Table 2 shows that the effluent and removal efficiency of COD and NH_4^+–N from POAGS in R1 system during the whole experimental process, compared with AAGS in R2 system. The mean COD removal efficiency from POAGS in R1 system reached to 82% but only 60% that from AAGS in R2 system, when the average influent load was 2.9 kgCOD m^{-3} d^{-1} (Tables 1 and 2). 83% of mean NH_4^+–N removal from POAGS in R1 system took place, 14% higher than that from AAGS in R2 system, when the mean influent loading of NH_4^+–N was 0.18 kg m^{-3} d^{-1} (Tables 1 and 2).

The correlation between influent concentration and effluent concentration in R1 and R2 was shown in Fig. S1. The effluent concentration of COD and NH_4^+–N from POAGS system was seldom affected by the fluctuated influent concentration due to the raw wastewater with the daily variation, compared with AAGS system at HOLR. That was attributed to the positive treatment ability of HOLR wastewater from the pure-oxygen aeration system [19–21]. The sufficient DO in R1 promoted formation of the compact granules to increase amount of microorganism biomass in R1 system (4.9 g MLSS L^{-1}). The biomass growth was conducive to microbial aggregates into POAGS that possessed the extraordinary tolerance to decompose the HOLR wastewater (Fig. S1). However, the fluffy AAGS was not beneficial to increase the microorganism biomass in R2 (3.4 g MLSS L^{-1}). In addition, another important reason was probably owing to the improved biomass activity by the higher oxygen transfer efficiency, for the greater saturation DO level of pure oxygen aeration than air aeration [19,22,23].

3.2. Settleability of POAGS

For clear expression of the distinct sludge settling performance from the different aeration source, the sludge

Table 1
Substrate composition, concentration and loading of synthetic wastewater for POAGS and AAGS cultivation

Substrate composition (mg L^{-1})				Influent concentration (mg L^{-1})		Influent loading (kg m^{-3} d^{-1})	
Glucose	NH_4Cl	KH_2PO_4	$CaCl_2$	COD	NH_4^+–N	COD	NH_4^+–N
2,000	200	100	20	960–2,640 (mean 1,845)	44–218 (mean 117)	1.5–4.1 (mean 2.9)	0.07–0.34 (mean 0.18)

Table 2
Effluent concentration and removal efficiencies in R1 and R2

Nutrients	R1 (POAGS) during the whole experimental process		R2 (AAGS) during the whole experimental process	
	Effluent concentration	Removal efficiencies (%)	Effluent concentration	Removal efficiencies (%)
COD (mg L^{-1})	1,680–40 (mean 334)	19–98 (mean 82)	1,840–80 (mean 746)	12–95 (mean 60)
NH_4^+–N (mg L^{-1})	115–3 (mean 17)	18–98 (mean 83)	78–2 (mean 31)	18–99 (mean 69)

settling height change with the settling time is shown in Fig. 2. There were same trends of the change of sludge settling height with time in the two bioreactors during the original stage of sludge cultivation (Fig. 2a). However, the apparent discrepancies were observed in the later sludge cultivation (Figs. 2b–d). There was a range of 18–48 cm of the altitude intercept (Δh) of sludge settling height between R1 and R2 based on the curves and fitting equations in Fig. 2. Besides, the sludge settling heights decreased exponentially with respect to settling time in the two bioreactors ($R^2 = 0.97$–0.99, $p < 0.01$). The results indicated that the excellent settling performance of POAGS in short time was more preferable to dispose the HOLR sewage. That was attributed to the adequate DO that is beneficial to microorganisms growth and aggregation [3,15,18], which could form stable and compact AGS to improve the settleability of sludge and allow an effective solid–liquid separation [35,37,38]. Additionally, the sludge settling velocity was studied by curve equation derivation (Fig. 2). The result appeared that the sludge settling velocity of R1 (6.8 m h^{-1}) was about three times higher than that of R2 (2.8 m h^{-1}). Thus, this indicated that the pure oxygen provided a high DO concentration which could influence the biomass activity that was conducive to form the dense and compact structure, which improved the sludge settling performance [35,38].

3.3. Biological morphologies of POAGS

The micromorphology of POAGS in R1 and AAGS in R2 was observed (Figs. 3a–h). The original sludge had a fluffy, irregular and loose-structure morphology with color of grayish and small size less than 0.2 mm [36]. The dense and large flocs with majority of bacteria aggregation appeared in R1 after 10 d (red circles in Figs. 3a–d), but the loose flocs were intertwined amounts of filamentous in R2 (red circles in Figs. 3e, f and g). This compact structure formation in R2 was delayed, as shown in Fig. 3h. Obviously, there was more abundant biomass in per POAGS than that in AAGS (Figs. 3a–h). Massive biomass growth in granules was beneficial to maintain high microorganism activities as well as EPS secretion under HOLR condition [8,13].

After 30 d, POAGS appeared in R1 and AAGS was formed in R2 (Figs. 3i–j). The granular sludge from R1 and R2 was not significantly disintegrated during the whole experiment. Obviously, POAGS from the R1 have a dense and compact structure with dark brown color (Fig. 3i), while the loose AAGS with yellow color were found in R2 (Fig. 3j). Actually, granular sludge is a heterogenous mixture of particles, microorganisms, colloids, EPS and cations [17]. The properties of individual granular sludge regulate the flocculation and dewatering characteristics of the biomass and the performance of solid–liquid separation in a bioreactor [17]. It has been found that the granular sludge with dense and compact structure has a strong stability to resist HOLR wastewater and enhance effluent water quality as well as sludge settle ability. The dense and compact granules might be related with the high DO concentration which would influence the bioactivity that excreted the EPS to benefit the bacteria aggregation and further form a stable sludge structure [39].

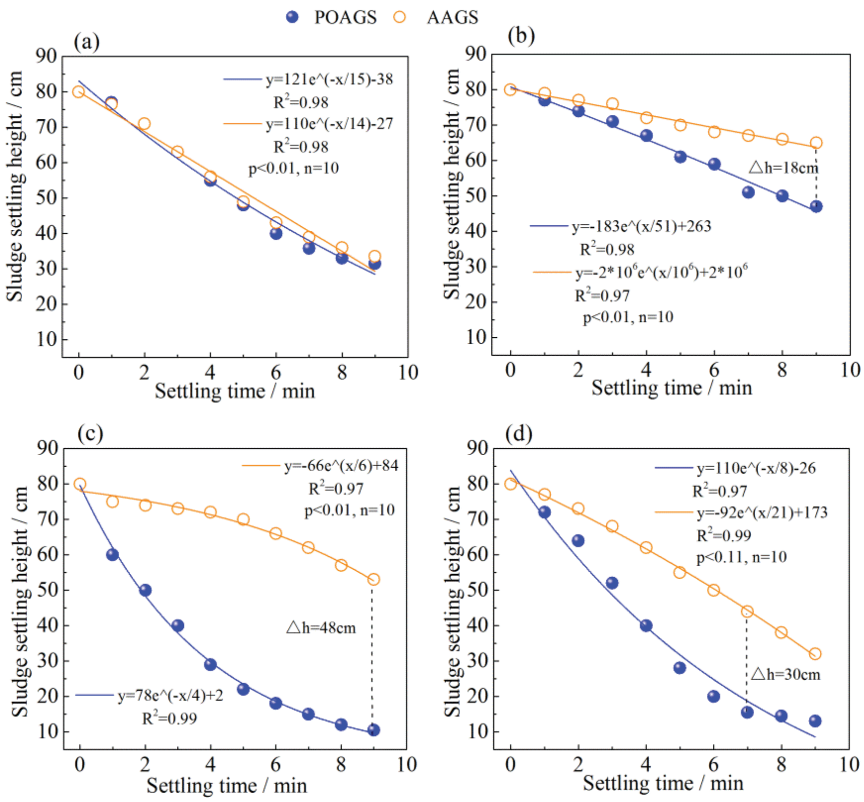

Fig. 2. Settling curves from initial cultivation (a), day 17 (b), day 24 (c) and day 48 (d) in R1 and R2.

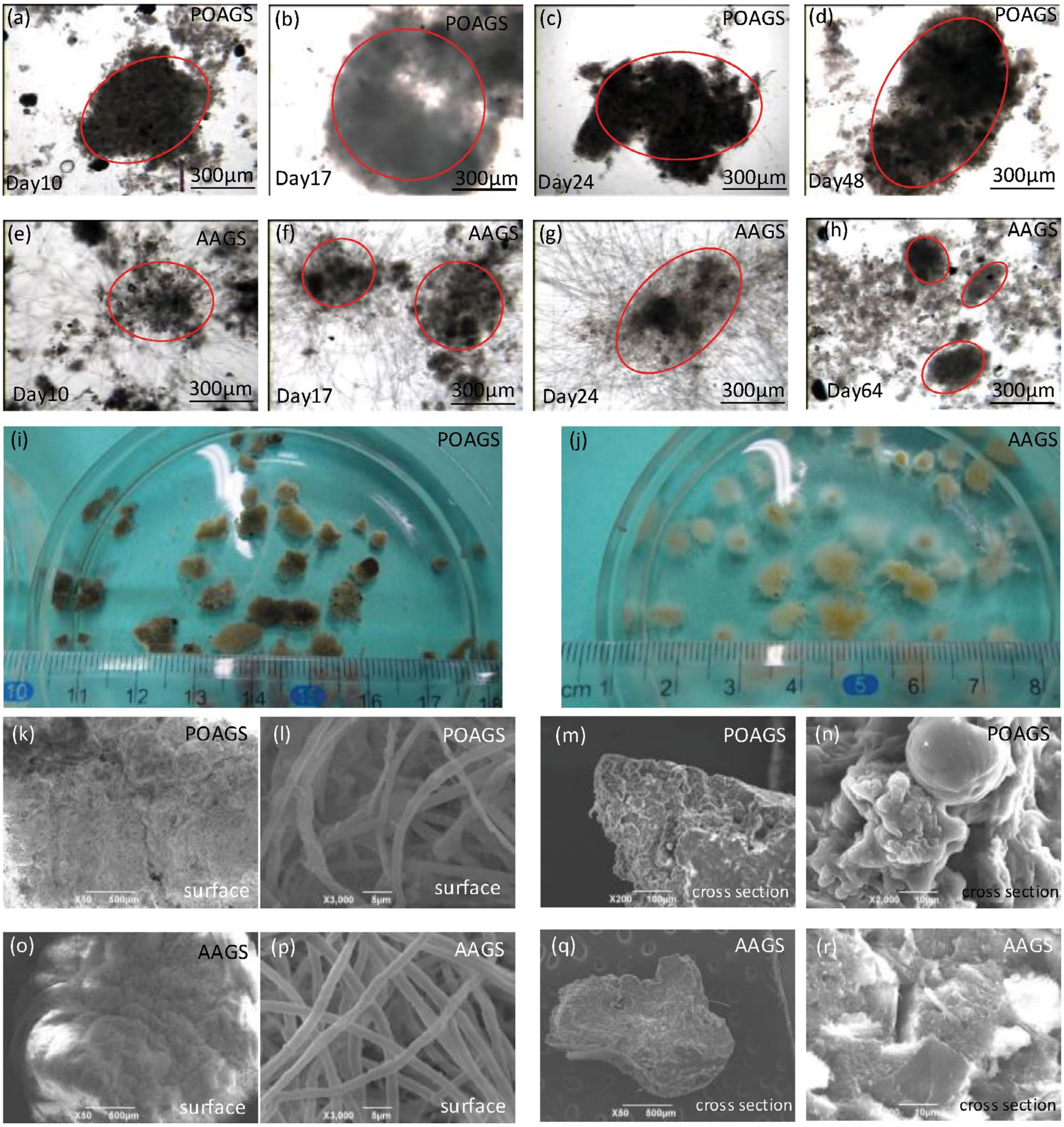

Fig. 3. Micromorpology of flocs about POAGS and AAGS in different periods observed by optical microsocpe (10× magnification) (a–h), image analysis of POAGS and AAGS (i,j) and scanning electron microgranph (SEM) of POAGS and AAGS taken from R1 and R2 in mature stage (k–r).

Detailed microstructures of the mature POAGS and mature AAGS were further monitored using SEM and are presented in Figs. 3k–r. Granular sludge with a clear round outer shape was formed in R1 and R2 (Figs. 3k and o). The granular surface was randomly selected to be further amplified (magnification ×3,000). It can be clearly seen that filamentous were still predominant in both POAGS and AAGS surface (Figs. 3l and p). When glucose served as exclusive carbon source was added in bioreactors, filamentous was easy to grow and entwine in the granules [10,39]. However, there seems to be more porosities and more abundant microorganisms in POAGS surface compared with those in AAGS surface (Figs. 3k, l, o and p).

Besides, the inner structure of POAGS and AAGS was presented in Figs. 3m, n, q and r. A very compact bacterial structure of POAGS, in which cells were tightly linked together and a rod-like species was found to be predominant when the inner structure was further magnified ×2,000 (Fig. 3n). Such a tight cellular structure was not found in the AAGS (Fig. 3r). That is due to higher porosity of POAGS surface that was beneficial to support DO transfer and nutrient uptake resulting in microorganisms growth inside the granules [8,40].

3.4. Mineral elements and functional groups of POAGS

Fig. 4a shows that the percentage of mineral elements' weight from POAGS, AAGS based on XRF measure. It was found that the mineral clusters of Ca, K, P and Cl occupied a large proportion in POAGS and AAGS, which might be related to substrate composition of the synthetic wastewater (Table 1). The presence of mineral clusters in the granules, concentrating all the calcium and kalium and considerable amounts of phosphorus, was consistent with the report by Angela et al. [4]. It was noticeable that the requirement of Ca from POAGS was less than that from AAGS, but more P can be assimilated by POAGS in Fig. 4a. That means the formation of POAGS demands less the addition of Ca^{2+} and eliminates more P in the wastewater. EDX coupled with SEM analyses was carried out on cut mature granules and typical images for central slices of POAGS and AAGS are shown in Figs. 4b and c. It was found that the elements of P, K and Ca occupied an important fraction of the total weight in POAGS, whereas the elements of C, Ca, O took up a main part of the total weight in AAGS.

The result indicated that the calcium element seems to play a critical role in POAGS and AAGS. Ca^{2+} was conducive to enhance granulation since inorganic ions were believed to neutralize the negative charge on the surface of bacteria [41]. Sajjad and Kim [6] showed that the addition of Ca^{2+} extremely enhanced the band intensity of O–H, suggesting the higher concentration EPS of microorganisms secretion. In addition, high DO stimulated the enrichment of polyphosphate accumulating organisms (PAO) favoring P biosorption and bioaccumulation [3,4], that might be the reason why more abundant P was accumulated in POAGS than in AAGS. The P coexisted with Ca in POAGS, it was possible to form hydroxyapatite and calcium phosphate [4], which was favorable for P removal of the high organic loading wastewater.

Fig. 4d shows that the functional groups of mature granules in R1 and R2 based on FTIR spectrometry. The spectra of POAGS and AAGS were similar and new characteristic peak did not appear in granules, probably owing to the identical seed sludge. The peak at 3,400 cm^{-1} was associated with the –OH stretching vibration and the peak at 2,930 cm^{-1} was related with $-CONH_2$ functional groups [42]. The peak at 1,650 cm^{-1} was connected with the C=O stretching vibration of β-sheets in secondary protein structures which existed in EPS that favored bio-flocculation [39,43]. The band at 1,400 cm^{-1} (–COO) existed in granular sludge and was caused by the symmetric stretching vibration of deprotonated carboxylic acid groups, which indicated the acidic nature of EPS components [12,39]. The peak at 1,060 cm^{-1} corresponding to carbohydrate between 1,200 and 1,000 cm^{-1} was associated with the vibrational stretching of O–H and C–O [9]. Abundant functionalities of sludge from POAGS and AAGS played an important role in high organic matter degradation. The presence of –COOR, –COOH, $-CONH_2$ and C=O (β-sheets) functionalities probably containing proteins, carbohydrates and alcohols promoted microbial aggregation [39].

3.5. DO, EPS and nutrients for POAGS formation and properties

POAGS have a denser and more compact structure, preferable removal efficiency, resistance to influent loading shock and excellent settleability compared with AAGS at HOLR, based on the experimental results. This might

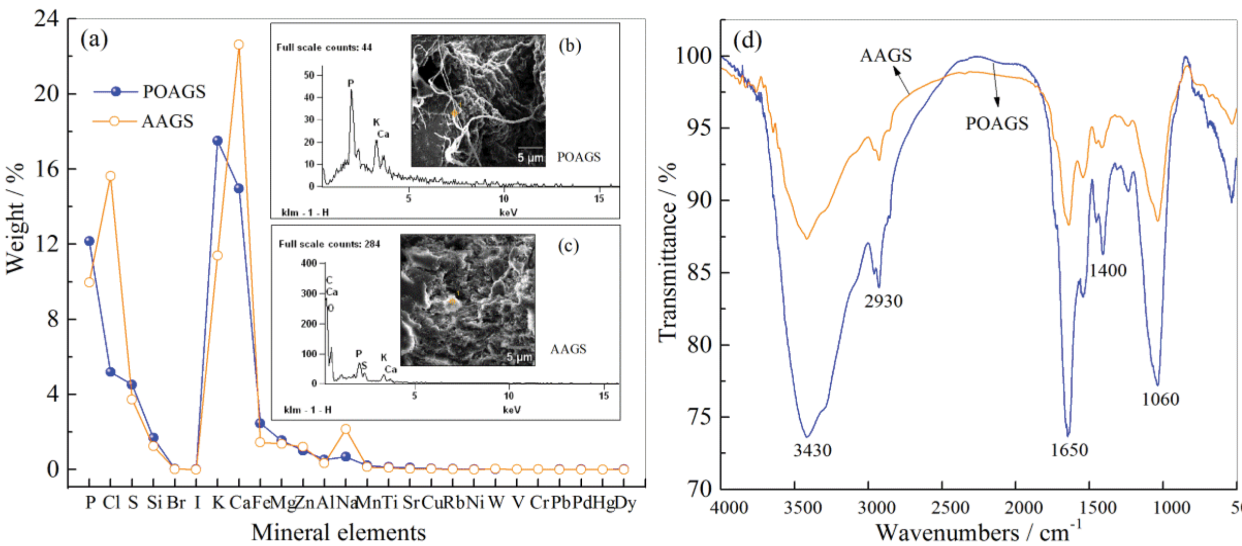

Fig. 4. Analysis of mineral elements and functional groups for POAGS and AAGS. (a) Percentage of mineral clusters' weight from POAGS and AAGS using XRF. (b), (c) Mineral elements and their counts from central slices of POAGS and AAGS using SEM-EDS. (d) Functional groups from POAGS and AAGS using FTIR.

be associated with higher DO in the pure aeration system compared with in the air aeration system (Fig. 5a), resulting in improvement of microorganism metabolic activity to promote the considerable amounts of EPS secretion for POAGS (Fig. 5b). The abundant EPS with strong viscosity in POAGS played role in adsorption, mass transfer, energy exchange, hydrophobicity and reducing granule surface charge to accelerate organic degradation [37,44,45].

The potential causes of high removal efficiency and excellent settleability for POAGS at HOLR can be further elucidated, as shown in Fig. 6. The dense and compact POAGS has a readily available in fast mass transfer in this work. The underlying reason was that the oxygen gas pressure in the pure oxygen aeration is almost five times higher than that of in the air aeration (Fig. 6a). Too compact regular microstructure or too looser filamentous microstructure of AAGS was appeared to limit mass transfer of nutrients and delayed the onset of diffusion limitation at HOLR [39]. After all, gas holdup is an important factor influencing the mass transfer of oxygen after onset speed [12]. For one thing, the gas holdup in POAGS is extremely higher than that in AAGS, when the oxygen transferred from the peripheral surface to the central zone of granule (P1 > P2, P3 > P4) (Figs. 5a and 6a). For another, the pressure differential of P1 and P3 for POAGS was higher than that of P5 of microorganism cell interior in pure oxygen aeration system (Fig. 6a). Therefore, those microorganisms were capable of obtaining adequate oxygen supply. However, the pressure differential of P4 for AAGS was lower than that of P5 of microorganism cell interior in air aeration (Fig. 6a). As a result, the internal microorganisms were difficult to obtain oxygen molecule for organics degradation of aerobic metabolism.

Due to the high-pressure differential in POAGS, the oxygen together with nutrients (organic matter) was transported to microorganism interior, resulting in large amounts of EPS secretion (Fig. 6b). Thus, the event of elastic swelling and shrinkage could occur because of the strong viscosity of the large quantity of EPS secretion. Meanwhile, some metabolic products were discharged outside of granule (Fig. 6c). It is a reasonable interpretation that POAGS was capable of possessing excellent physiochemical and biological properties, when AGS process treating HOLR wastewater was combined with pure oxygen aeration technology [13,14,20].

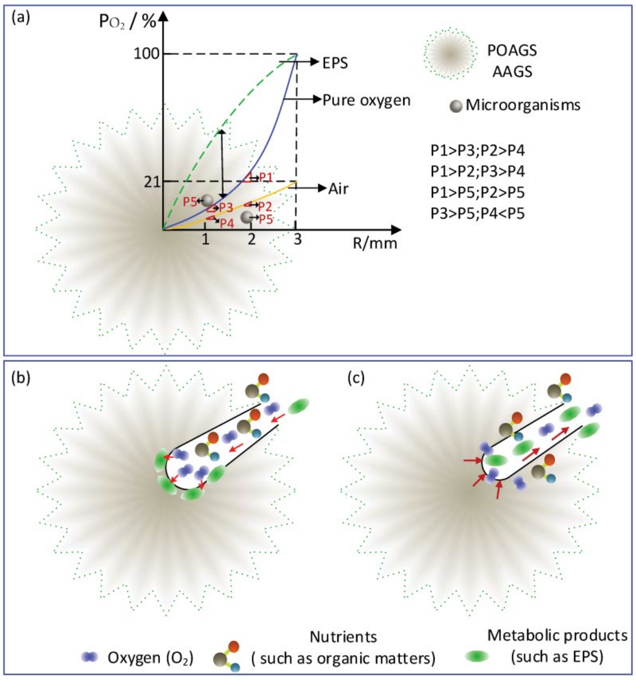

Fig. 6. Oxygen pressure discrepancy between POAGS and AAGS in mass transfer process (P1, P3 are the oxygen pressure discrepancies under 1 and 2 cm radius from POAGS, respectively; P2, P4 are the oxygen pressure discrepancies under 1 and 2 cm radius from AAGS, respectively; P5 under 1 and 2 cm radius from microorganism of POAGS and AAGS, respectively) (a), internal transportation of oxygen and nutrients (b) and external transport of metabolic products (c) from POAGS.

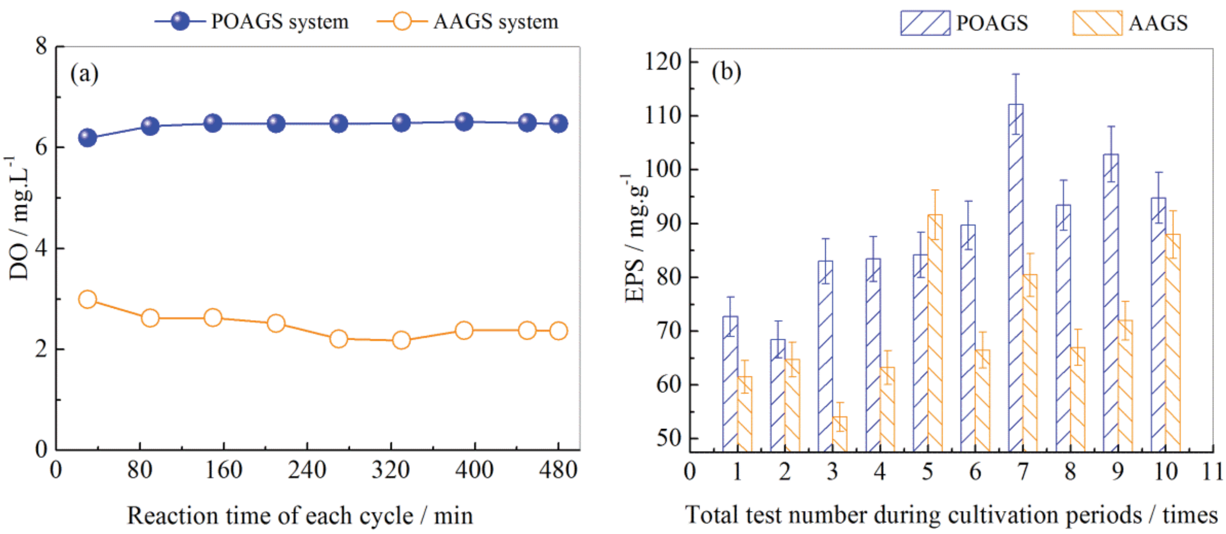

Fig. 5. DO concentration with reaction time of each cycle (a), EPS content from POAGS and AAGS during cultivation (b).

4. Conclusion

The physiochemical and biochemical properties of POAGS treating HOLR wastewater in contrast with AAGS were investigated in this study. The result indicated that removal rate of COD and NH_4^+–N for POAGS was separately 22% and 14% higher compared with that for AAGS at mean influent loading of 2.9 COD kg m^{-3} d^{-1} and 0.18 NH_4^+–N kg m^{-3} d^{-1}. Meanwhile, POAGS has a strong resistance under HOLR resulting in the effluent, which was less influenced by the high influent loading. The investigation of settling curves showed that sludge settling performance of POAGS was better than that of AAGS. And the sludge settling velocity of POAGS was three times as fast as that of AAGS, under HOLR. The compacted structure existed in POAGS could aggregate the multi-species community of microorganisms secreting abundant viscous EPS compared with the loose structure in AAGS. The formation of POAGS was capable of requiring less the addition of Ca^{2+} and absorbing more P from the wastewater than that of AAGS. Additionally, abundant functionalities of sludge from POAGS played an important role in high organic matter degradation. This came along with great benefits in terms of maintaining stable removal efficiency and prominent settling ability involved under HOLR. It was further speculating that the combined action of adequate DO and rich nutrient was a prerequisite for the formation of excellent physiochemical and biochemical properties in POAGS.

Acknowledgments

The author acknowledges the financial support from the National Natural Science Foundation of China (No. 31070401), the College Natural Science Foundation of Major Project of Anhui, China (KJ2018ZD033), the Foundation of Provincial Key Laboratory of Biotic Environment and Ecological Safety in Anhui.

References

[1] T.B. Mao, B. Yu, C. Wu, Research advances on the high-strength organic wastewater treatment, Adv. Mater. Res., 550–553 (2012) 2407–2411.
[2] S. Wang, I. Savva, R. Bakke, A full-scale hybrid vertical anaerobic and aerobic biofilm wastewater treatment system: case study, Water Pract. Technol., 14 (2019) 189–197.
[3] S.L.D.S. Rollemberg, A.R.M. Barros, P.I.M. Firmino, A.B.D. Santos, Aerobic granular sludge: cultivation parameters and removal mechanisms, Bioresour. Technol., 270 (2018) 678–688.
[4] M. Angela, B. Beatrice, S. Mathieu, Biologically induced phosphorus precipitation in aerobic granular sludge process, Water Res., 45 (2011) 3776–3786.
[5] N.A. Awang, M.G. Shaaban, Effect of reactor height/diameter ratio and organic loading rate on formation of aerobic granular sludge in sewage treatment, Int. Biodeterior. Biodegrad., 112 (2016) 1–11.
[6] M. Sajjad, K.S. Kim, Studies on the interactions of Ca^{2+} and Mg^{2+} with EPS and their role in determining the physicochemical characteristics of granular sludges in SBR system, Process Biochem., 50 (2015) 966–972.
[7] S.Y. Liu, G. Liu, Y.C. Tian, Y.P. Chen, H.Q. Yu, F. Fang, An innovative microelectrode fabricated using photolithography for measuring dissolved oxygen distribution in aerobic granules, Environ. Sci. Technol., 41 (2007) 5447–5452.
[8] B.S. McSwain, R.L. Irvine, M. Hausner, P.A. Wilderer, Composition and distribution of extracellular polymeric substances in aerobic flocs and granular sludge, Appl. Environ. Microb., 71 (2005) 1051–1057.
[9] S. Milia, E. Malloci, A. Carucci, Aerobic granulation with petrochemical wastewater in a sequencing batch reactor under different operating conditions, Desal. Wat. Treat., 57 (2016) 27978–27987.
[10] J.H. Tay, Q.S. Liu, Y. Liu, Microscopic observation of aerobic granulation in sequential aerobic sludge blanket reactor, J. Appl. Microbiol., 91 (2001) 168–175.
[11] S.K. Toh, J.H. Tay, B.Y. Moy, V. Ivanov, S.T. Tay, Size-effect on the physical characteristics of the aerobic granule in a SBR, Appl. Microbiol. Biotechnol., 60 (2003) 687–695.
[12] L. Zhu, H.Y. Qi, M.L. Lv, Y. Kong, Y.W. Yu, X.Y. Xu, Component analysis of extracellular polymeric substances (EPS) during aerobic sludge granulation using FTIR and 3D-EEM technologies, Bioresour. Technol., 124 (2012) 455–459.
[13] B.X. Thanh, C. Visvanathan, R.B. Aim, Characterization of aerobic granular sludge at various organic loading rates, Process Biochem., 44 (2009) 242–245.
[14] C. Caudan, A. Filali, M. Sperandio, E. Girbal-Neuhauser, Multiple EPS interactions involved in the cohesion and structure of aerobic granules, Chemosphere, 117 (2014) 262–270.
[15] H.L. Zhang, W.L. Jiang, R. Liu, Y. Zhou, Y. Zhang, Organic degradation and extracellular products of pure oxygen aerated activated sludge under different F/M conditions, Bioresour. Technol., 279 (2019) 189–194.
[16] L. Amand, B. Carlsson, Optimal aeration control in a nitrifying activated sludge process, Water Res., 46 (2012) 2101–2110.
[17] G.P. Sheng, H.Q. Yu, X.Y. Li, Stability of sludge flocs under shear conditions, Biochem. Eng. J., 38 (2008) 302–308.
[18] S. Kundral, R. Mudragada, E. Coro, M. Moncholi, N. Mora, S. Laha, B. Tansel, Improving settling characteristics of pure oxygen activated sludge by stripping of carbon dioxide, Water Environ. Res., 87 (2015) 498–505.
[19] H.F. Zhuang, X.T. Hong, H.J. Han, S.D. Shan, Effect of pure oxygen fine bubbles on the organic matter removal and bacterial community evolution treating coal gasification wastewater by membrane bioreactor, Bioresour. Technol., 221 (2016) 262–269.
[20] F.A. Rodríguez, P. Reboleiro-Rivas, J. Gonzalez-Lopez, E. Hontoria, J.M. Poyatos, Comparative study of the use of pure oxygen and air in the nitrification of a MBR system used for wastewater treatment, Bioresour. Technol., 121 (2012) 205–211.
[21] F.A. Rodríguez, J.M. Poyatos, P. Reboleiro-Rivas, F. Osorio, J. Gonzalez-Lopez, E. Hontoria, Kinetic study and oxygen transfer efficiency evaluation using respirometric methods in a submerged membrane bioreactor using pure oxygen to supply the aerobic conditions, Bioresour. Technol., 102 (2011) 6013–6018.
[22] F.A. Rodríguez, M.V. Martinez-Toledo, J. Gonzalez-Lopez, E. Hontoria, J.M. Poyatos, Performance of bench-scale membrane bioreactor under real work conditions using pure oxygen: viscosity and oxygen transfer analysis, Bioprocess Biosyst. Eng., 33 (2010) 885–892.
[23] K. Calderon, A. Gonzalez-Martinez, C. Montero-Puente, P. Reboleiro-Rivas, J.M. Poyatos, B. Juarez-Jimenez, M.V. Martinez-Toledo, B. Rodelas, Bacterial community structure and enzyme activities in a membrane bioreactor (MBR) using pure oxygen as an aeration source, Bioresour. Technol., 103 (2012) 87–94.
[24] P. Jiang, C.J. Tzeng, C.C. Hsieh, M.K. Stenstrom, Modeling VOC emissions in the high-purity oxygen activated sludge process, J. Environ. Eng., 136 (2010) 1189–1196.
[25] H.W. Zhu, T.C. Keener, P.L. Bishop, T.L. Orton, M. Wang, K.F. Siddiqui, Aeration recirculation in air and high purity oxygen systems for control of VOC emissions from wastewater aeration basins, Environ. Prog., 18 (1999) 101–106.
[26] J.K. Nelson, J.L. Puntenney, Performance comparison of the air and high-purity-oxygen activated sludge system, J. Water Pollut. Control Fed., 55 (1983) 336–340.
[27] T.W. Barber, K.I. Ashley, D.S. Mavinic, K. Christison, Superoxygenation: analysis of oxygen transfer design parameters using high-purity oxygen and a pressurized column, Can. J. Civil Eng., 42 (2015) 737–746.

[28] G.M. Neerackal, P.M. Ndegwa, H.S. Joo, X. Wang, C.S. Frear, J.H. Harrison, M.W. Beutel, Potential application of *Alcaligenes faecalis* strain No. 4 in mitigating ammonia emissions from dairy wastewater, Bioresour. Technol., 206 (2016) 36–42.
[29] N.K. Shammas, L.K. Wang, In: L.K. Wang, Biological Treatment Processes, Humana Press, a part of Springer Science+Business Media, LLC, USA, 2009, pp. 283–333.
[30] C.J. Tzeng, R. Iranpour, M.K. Stenstrom, Modelling and control of oxygen transfer in high purity oxygen activated sludge process, J. Environ. Eng., 129 (2003) 402–411.
[31] W.H. Dong, J. Yang, S.F. Zhang, N. Li, Progress of the Research on Pure Oxygen Aeration, China Resour. Compr. Util., 24 (2006) 28–30 (in Chinese with an English abstract).
[32] Z.T. Chen, S.G. Li, G.Y. Han, Y.C. Xie, Application of micro-bubble pure oxygen aeration technique to the treatment of industrial wastewater, Ind. Water Treat., 28 (2008) 13–16 (in Chinese with an English abstract).
[33] APHA, Standard Methods for the Examination of Water and Wastewater, 12 ed. American Public Health Association, Washington DC, 1998.
[34] D. Zhang, Z. Li, P. Lu, T. Zhang, D. Xu, A method for characterizing the complete settling process of activated sludge, Water Res., 40 (2006) 2637–2644.
[35] A.J. Schuler, H. Jang, Density effects on activated sludge zone settling velocities, Water Res., 41 (2007) 1814–1822.
[36] F.H. Pan, Y.B. Jiang, K.X. Huang, X.X. Zhang, Y.J. Huang, X.Y. Wang, Potential causes of high performance of pure-oxygen aerobic granules in SBR under high organic loading condition, Global Nest J., 19 (2017) 687–696.
[37] B.Q. Liao, H.J. Lin, S.P. Langevin, W.J. Gao, G.G. Leppard, Effects of temperature and dissolved oxygen on sludge properties and their role in bioflocculation and settling, Water Res., 45 (2011) 509–520.
[38] B.M. Wilen, D. Lumley, A. Mattsson, T. Mino, Relationship between floc composition and flocculation and settling properties studied at a full scale activated sludge plant, Water Res., 42 (2008) 4404–4418.
[39] A.R. Badireddy, S. Chellam, P.L. Gassman, M.H. Engelhard, A.S. Lea, K.M. Rosso, Role of extracellular polymeric substances in bioflocculation of activated sludge microorganisms under glucose-controlled conditions, Water Res., 44 (2010) 4505–4516.
[40] H. Liu, H.H.P. Fang, Hydrogen production from wastewater by acidogenic granular sludge, Water Sci. Technol., 47 (2003) 153–158.
[41] I. Othman, A.N. Anuar, Z. Ujang, N.H. Rosman, H. Harun, S. Chelliapan, Livestock wastewater treatment using aerobic granular sludge, Bioresour. Technol., 133 (2013) 630–634.
[42] J. Schmitt, H.C. Flemming, FTIR-spectroscopy in microbial and material analysis, Int. Biodeterior. Biodegrad., 41 (1998) 1–11.
[43] A. Jouraiphy, S. Amir, P. Winterton, M. El Gharous, J.C. Revel, M. Hafidi, Structural study of the fulvic fraction during composting of activated sludge-plant matter: elemental analysis, FTIR and 13C NMR, Bioresour. Technol., 99 (2008) 1066–1072.
[44] B.Y.P. Moy, J.H. Tay, S.K. Toh, Y. Liu, S.T.L. Tay, High organic loading influences the physical characteristics of aerobic sludge granules, Lett. Appl. Microbiol., 34 (2002) 407–412.
[45] P. Yan, R.C. Qin, J.S. Guo, Q. Yu, Z. Li, Y.P. Chen, Y. Shen, F. Fang, Net-zero-energy model for sustainable wastewater treatment, Environ. Sci. Technol., 51 (2017) 1017–1023.

Supplementary information:

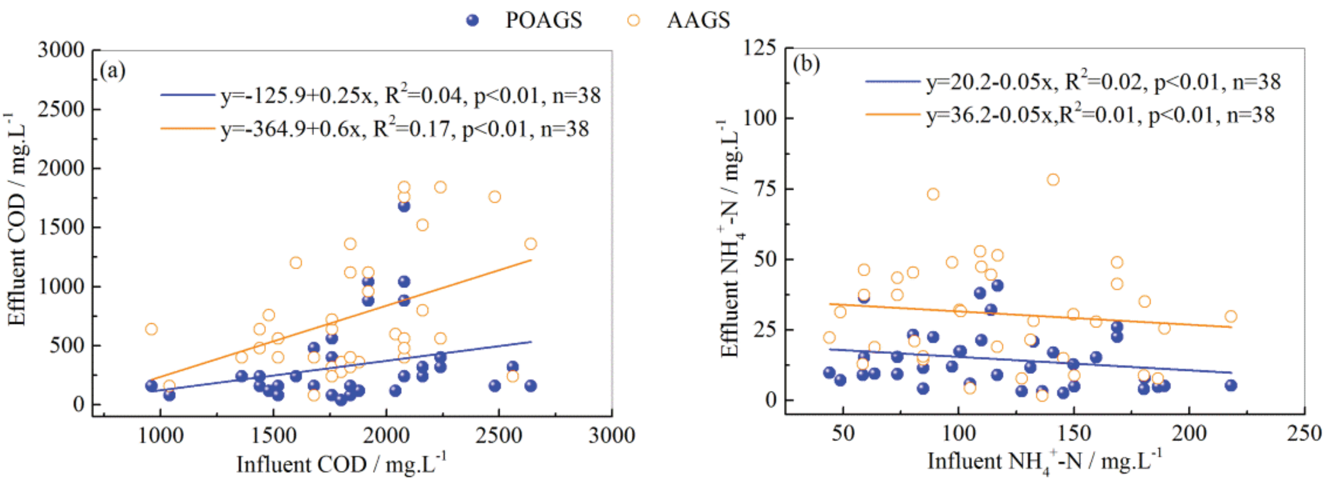

Fig. S1. Correlation analysis between influent COD and effluent COD (a) and between influent NH_4^+–N and effluent NH_4^+–N (b) in R1 and R2.